Research Article

Characterization of Home Range Using Point Peeling Algorithms

SUE K. BATH,[1] *School of Industrial and Systems Engineering, Georgia Institute of Technology, Atlanta, GA 30332-0205, USA*
ANTHONY J. HAYTER, *School of Industrial and Systems Engineering, Georgia Institute of Technology, Atlanta, GA 30332-0205, USA*
DAVID A. CAIRNS,[2] *Department of Probability and Statistics, University of Sheffield, Sheffield, S10 2TN, UK*
CARL ANDERSON,[3] *School of Industrial and Systems Engineering, Georgia Institute of Technology, Atlanta, GA 30332-0205, USA*

Abstract

Many statistical procedures and metrics have been developed to analyze animal home-range data. We evaluated a point peeling method that may be useful in the analysis of such data. Our objectives were to 1) identify an appropriate peeling criterion that performs well across the suite of underlying behaviors, and 2) compare sample and expected utilization distribution (UD) curves as the basis of a procedure for classifying animal behavior. We addressed the first objective by comparing 3 peeling criteria: 1) peeling farthest from the sample centroid, 2) peeling farthest from the harmonic mean, and 3) peeling the location that caused the greatest decrease in area of remaining data. We compared these criteria across 5 different biologically plausible home-range behaviors as represented by 5 idealized statistical distributions. Comparison of expected UD curves and those generated from simulated data revealed several important considerations: 1) the centroid peeler offered the most accurate and consistent results, 2) the harmonic mean peeler exhibited particularly large amounts of variability, and 3) the area peeler was not able to consistently identify distributions representing clustered or territorial behavior. We addressed the second objective by comparing sample curves to expected UD curves using the centroid peeler. Results revealed each of the sample UD curves captured the key features of the underlying statistical distribution and hence, when dealing with real samples, the behavior. Further, in several examples, the UD curves identified underlying distributions that were not apparent by visual inspection. Overall, point peeling using the centroid peeling function provided a simple but robust procedure for field biologists that made good use of all the data from a sample. This procedure provided an objective home-range measure and a way of classifying home-range use. (THE JOURNAL OF WILDLIFE MANAGEMENT 70(2):422–434; 2006)

Key words

biotelemetry, convex hulls, home-range analysis, point peeling.

Biologists, especially behavioral ecologists and conservation biologists, have long been interested in the movement of animals in their habitat. Analysis of such movement may provide insights into an animal's (or group's) behavior and, especially in the case of threatened or endangered species, their needs in terms of habitat size, shape, and type. In the past, biologists have often relied upon traps and sightings to analyze movement, but these methods may not be representative of an animal's typical use of an area. The advent of radiotelemetry (e.g., Kenward 1987, 2001) in which reasonably accurate readings can be taken at regular intervals, even if the biologist cannot see the animal(s) they are tracking, has provided a higher level of objectivity and rigor. Once the data has been collected, however, we are still faced with the problem of how to analyze it. Many different statistical procedures and metrics have been developed to estimate home range, partly due to the lack of specificity of the term home range.

Burt (1943:351) was among the first to define formally an animal's home range: "... that area traversed by the individual in its normal activities of food gathering, mating, and caring for young. Occasional sallies outside the area, perhaps exploratory in nature, should not be considered part of the home range." This definition, while conceptually clear, is often difficult to quantify. First, the term normal is highly ambiguous. Second, and related, it is difficult to quantify the term occasional sallies. Should such ventures be defined as a percentage of the outer home-range area or a small number of extreme outliers or some other plausible interpretation? More recent definitions incorporate greater objectivity; e.g., the notions of center of activity and core area (Hayne 1949, Hodder et al. 1998, Kernohan et al. 2001) that generally refer to a central area in which the animal can most likely be found. However, there are still problems. Core areas may be mono- or poly-nuclear (reviewed in Wray et al. 1992), and there is still subjectivity in the proportion of locations of the sample that are considered extreme and therefore eliminated from the sample for analysis. For instance, taking only the central 50% of locations (e.g., Worton 1995) is statistically robust, but this method may be excessively harsh, especially for field studies with small sample sizes.

One approach (reviewed in Kenward 1987, 2001, White and Garrott 1990, Kernohan et al. 2001) that involves using all of the available data (see below) is to peel individual locations from the sample according to some criterion and then estimate home range for that sample as the area of the minimum convex polygon (MCP) of the remaining data. Multiple semi-objective home-range estimates (e.g., the 95 and 100% home-ranges areas [Van Stralen 1998]) can be obtained by plotting MCP area versus proportion of sample comprising that area—known as the utilization distribution (UD) curve. The shape of this UD curve, which we normalized for ease of comparison among samples, may provide a way to assess how the animal uses its home range; for instance, spending a disproportionate amount of time at the boundaries possibly indicates territorial or pseudoterritorial behavior (cf. Stewart et al. 1997, Hatchwell et al. 2001).

Our objective was to examine the above peeling method in

[1] *E-mail: sbath@isye.gatech.edu*
[2] *Present address: Cancer Research UK Clinical Centre, St. James's University Hospital, Leeds, LS9 7TF, UK*
[3] *Present address: Qbit, LLC., 6905 Rockledge Drive, 3rd Floor, Bethesda, MD 20817, USA*

more detail because, as Boulanger and White (1990:315) state: "... proposed estimators should be tested through simulation studies to demonstrate their operating characteristics." While the idea of peeling individual locations from samples is not new (e.g., Kenward 1987), previous analysis of the method has been very preliminary. For instance, although various criteria were proposed for deciding which location should be removed at each stage (e.g., the location farthest from the sample's centroid), little rigorous comparison among these criteria has been performed (but see Boulanger and White 1990). Further, it is not clear how this point peeling technique fares on samples from animals with differing behavior and hence underlying distributions. For instance, while 1 criterion may perform well on samples from central place foragers, it may perform less well for highly territorial animals.

We are not advocating that the point peeling methods are necessarily the best out of all possible methods. In some situations kernel methods may be more appropriate or have better statistical properties (e.g., Seaman and Powell 1996, Powell 2000). Our point, however, is that point peeling methods have been and are used to quantify home range, and as Getz and Wilmers (2004:494) state: "... minimum convex polygons (MCP) and kernel methods are the mainstay of the home-range construction literature." More importantly, our systematic examination of the method's properties, or its operating characteristics, is precisely the objective information required to choose if and whether other methods (i.e., the use of kernels) have better statistical properties given a certain underlying behavior.

To achieve our goal, we idealized the range of animal behavior typically observed in radio-tracking studies into 5 classes: uniform or random, central place foraging, territorial, skewed central place foraging, and poly-nuclear activity. These are, in turn, idealized by 5 statistical distributions that would generate meaningful data (fix) samples if the animal were exhibiting that behavior. These distributions are uniform on a disk, bivariate normal, inverted bivariate normal, skewed bivariate, and multilocus clustered distribution respectively (Fig. 1; cf. Boulanger and White 1990). While we appreciate that no animal will conform exactly to these idealized distributions, they represent realistic base cases to which field data samples can be compared objectively. We are well aware that most animals will generate a sample of fixes that are somehow intermediate to these extreme cases, but it is useful to state objectively that a particular sample more closely matches that expected from, e.g., a skewed bivariate normal distribution than a circular bivariate normal distribution. Focusing on this point peeling method, we contrasted and tested 3 criteria with which to peel individual points from the sample: 1) farthest in distance from the centroid, 2) farthest from the harmonic mean center, and 3) the location that causes the greatest decrease in MCP area (see White and Garrott 1990, Anderson 1998, Hatchwell et al. 2001, Kernohan et al. 2001 for some pros and cons of using MCPs). We simulated samples from each of these distributions and tested them against each of the 3 peeling criterions. Our aim was 3-fold: 1) identify an appropriate peeling criterion that performed well (or poorly) across the whole suite of underlying behavior field biologists are likely to encounter, 2) compare the sample and expected UD curves as the basis of a procedure for classifying animal behavior and home-range use in a reasonably objective manner, and 3) illustrate our ideas with empirical data from several field studies using our 5 statistical distributions. Our overall goal was to provide a simple but robust

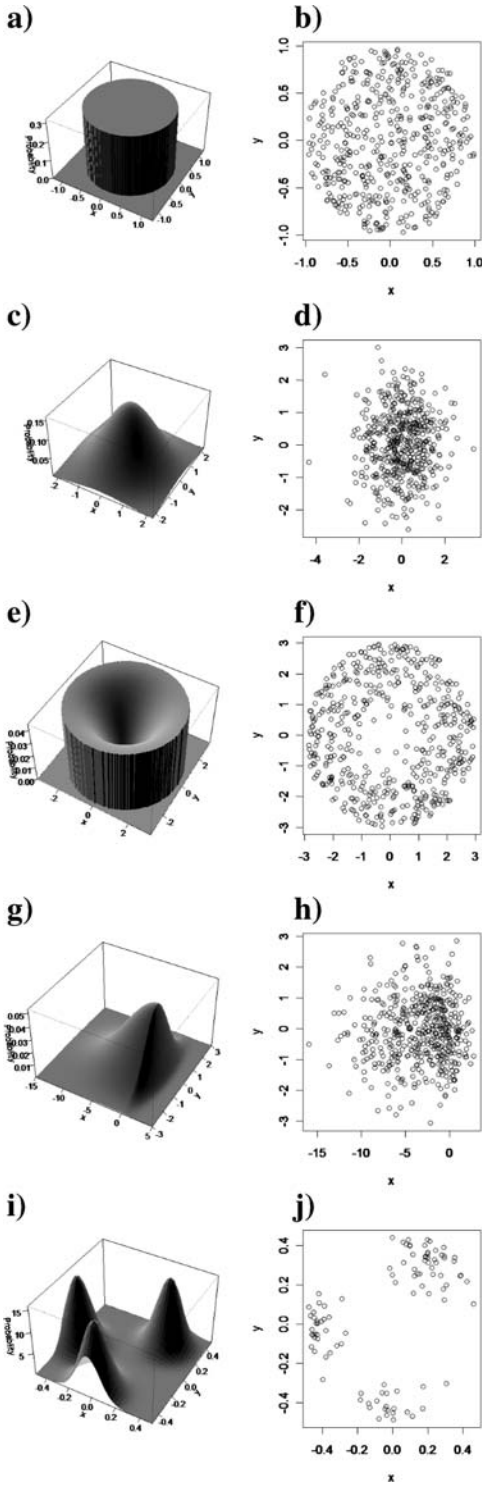

Figure 1. Illustrations and samples of the 5 idealized distributions: (a) and (b) base case: uniform on a disk; (c) and (d) central place foragers: bivariate normal; (e) and (f) territorial: inverted bivariate normal; (g) and (h) skewed central place foragers: skewed distribution with $\alpha = 5$ (increasing α smears the distribution farther to left); (i) and (j) polynuclear activity: multilocus clustered distribution ($\lambda = 2$, $\sigma = 0.1$, $\mu = 50$; smaller σ generates more concentrated clusters).

procedure for field biologists that makes good use of all the data from a sample (unlike the common practice of using only the 100% MCP that only uses the most extreme locations) and provides an objective measure of home range and classification of home-range use.

Idealized Animal Dispersion

Different home-range analysis techniques are more suited to some animal behavior, and hence classes of sample distributions, than others. To investigate this, we considered some of the major categories of behavior that may occur in study animals, and we idealized these behavioral categories in 5 different statistical distributions. In the following section, we set out the justification for each behavior and its associated idealized distribution. We ran our simulations in S-PLUS® (Version 6.1.2; Insightful Corporation, Seattle, Washington) and R (http://www.r-project.org/; Appendix A). Our analysis techniques are meant as a practical tool for field biologists; our primary motivation for the following distributions is biological, not mathematical.

Base Case: Uniform on a Disk

The simplest scenario is equal and unbiased habitat usage or visitation across the whole home range, thereby implying a uniform distribution. Uniform home-range usage may be exhibited by grazers or an animal essentially performing a random walk over a long time scale. In addition, the uniform distribution also represents randomly generated fixes across an area; therefore, it represents an important base case. The uniform distribution on a disk (Fig. 1a; Fig. 1b with sample size 500), here on a unit disk, has a joint probability density function (hereafter pdf):

$$f(x,y) = \begin{cases} \frac{1}{\pi} & \text{if } x^2 + y^2 \le 1 \\ 0 & \text{otherwise.} \end{cases} \quad (1)$$

Central Place Foragers: Bivariate Normal

Many animals are central place foragers, returning regularly to a core location such as nest, den, or roost site (Orians and Pearson 1979, Stephens and Krebs 1986). Generally, the probability of a fix decreases with increasing distance from the core location. This can be idealized (Fig. 1c; Fig. 1d with sample size 500) with a standard bivariate normal:
$N(\mu_1 = \mu_2 = 0, \sigma_1 = \sigma_2 = 1, \rho = 0)$ with joint pdf:

$$f(x,y) = \frac{1}{2\pi}\exp\left\{-\frac{1}{2}(x^2 + y^2)\right\} \quad (2)$$

and covariance matrix $\begin{bmatrix} 1 & 0 \\ 0 & 1 \end{bmatrix}$.

Territorial: Inverted Bivariate Normal

Some animals, and groups of animals, are territorial, spending a disproportion amount of time at the boundaries of their home ranges (Alcock 1998). They may actively patrol and defend their territory or pseudo-territorial behavior may arise for other reasons such as food dispersion (Stewart et al. 1997). Related, but not a home range, the territorial behavior of lekking animals (Gibson and Bradbury 1987 and references therein) can exhibit similar properties.

We idealized such behavior with an inverted bivariate normal distribution (Fig. 1e; Fig. 1f with sample size 500), bounded at radius σ from the origin (where $\sigma > 0$). That is:

$$\text{Let } c = 2\pi\left(\exp\left(-\frac{\sigma^2}{2}\right) + \frac{\sigma^2}{2} - 1\right). \quad (3)$$

$$f(x,y) = \frac{1}{c}\left(1 - \exp\left\{-\frac{1}{2}(x^2 + y^2)\right\}\right) \text{ for } x^2 + y^2 \le \sigma^2. \quad (4)$$

We took $\sigma = 3$, the equivalent of the central 98.89% of a bivariate normal distribution.

Skewed Central Place Foragers: Skewed Distribution

An animal's utilization distribution need not be rotationally symmetric. First, it may be elongated (idealized as elliptical) if the animal preferentially forages along 1 axis, say x. This may be applicable, for instance, to individuals in riparian (i.e., riverside) habitats. Second, as we simulated, the distribution may be asymmetrically skewed, say foraging preferentially in positive x than negative x (Fig. 1g for $\alpha = 5$; Fig. 1h with sample size 500). This may occur when there is some underlying gradient of habitat quality, such as elevation and temperature (e.g., at a valley's end), pollution, food density at the margin of a prey's distribution, etc.

We idealize this with a combination of 2 bivariate normal distributions: for positive x, a standard bivariate normal (as above), and for negative x:
$N(\mu_1 = \mu_2 = 0, \sigma_1 = \alpha, \sigma_2 = 1, \rho = 0)$ with $\alpha > 1$. The joint pdf is defined as:

$$f(x,y) = \begin{cases} \frac{1}{\pi(\alpha+1)}\exp\left\{-\frac{1}{2}(x^2 + y^2)\right\} & \text{for } x \ge 0 \\ \frac{1}{\pi(\alpha+1)}\exp\left\{-\frac{1}{2}\left(\frac{x^2}{\alpha^2} + y^2\right)\right\} & \text{for } x < 0. \end{cases} \quad (5)$$

It can be shown that the centroid of this skewed distribution is:

$$\left(\sqrt{2/\pi}(1 - \alpha^2)/(\alpha + 1), 0\right). \quad (6)$$

Polynuclear Activity: Multilocus Clustered Distribution

An animal's dispersion may often consist of multiple clusters. For instance, on a short timescale, a bird may fly to a group of bushes and spend a few minutes hopping from one branch to another, thus generating 1 group of fixes. The bird may then fly across the field to a second group of bushes or a hedge, spend some time foraging there, move on, and so on. On a longer timescale and larger spatial scale, this may represent dispersal or migratory behavior or nomadic species that spend a certain amount of time as central place foragers in 1 location, and who then move to a new location when the local resources have been depleted. An example is that of army ants (*Eciton* spp.) during their statary phase when the colony camps out in a single location for about 20 days, raiding the surrounding forest for food about 14 times during this period; the colony then enters its nomadic phase in which it camps out in a different location each day for about 15 days (Franks 1989).

We idealize these sorts of behavior with a 2-stage point process. First, a Poisson process with rate λ generated a set of parent locations in a plane. These locations were then used as the centers for a set of bivariate normal distributions, each with standard deviation $\sigma = \sigma_1 = \sigma_2$, from which the clusters of points, mean μ per cluster, were generated. This is known as the Thomas cluster process, a special case of the Neyman-Scott process, that we simulated using the rThomas routine of the SPATSTAT library (Baddeley and Turner 2005). From the center of this plane, we took a disk of sufficient radius such that it contained n locations. In other words, we ordered the locations in terms of increasing Euclidean distance from the center, and the sample consisted of the central n locations (Fig. 1i; Fig. 1j with sample size 500).

Utilization Distribution Curves and Point Peeling

In this section, we briefly outline the process and some expected characteristics of peeling individual locations from data. Although this is not a new procedure (Kenward 1987), we discuss some statistical properties not previously considered.

UD Curves

By peeling individual points, we mean an iterative process in which an individual location is selected according to some criterion and then removed from the data set. For each iteration, we calculated the area of the MCP of the remaining data. There are 2 main uses for this procedure. First, to eliminate the outer x% of locations, thus removing the outliers and most extreme data. Second, we can plot the utilization distribution (i.e., a curve of the proportion of points versus area [Ford and Krumme 1979, Kenward 1987]) that can help determine a core area or the overall distribution.

There are many possible criteria with which to select locations for removal. Practically, the most sensible criterion is to remove points farthest in Euclidean distance from any nest, den, or other habitation to which the animal regularly returns. Although there are others that we could have chosen (Kenward 1987), we considered 3 criteria: 1) location farthest in distance from centroid (arithmetic mean), 2) location farthest in distance from harmonic mean, and 3) location that caused greatest reduction in area.

Peeling from centroid.—The basis of this algorithm is simple and straightforward: 1) let $c = (\bar{x}, \bar{y})$ where n is the number of data points, 2) calculate area of the MCP of all remaining data, 3) select location farthest in distance from c, and 4) remove it from the data, repeat steps 2, 3, and 4 until as many points as desired have been peeled.

Peeling from harmonic mean.—Dixon and Chapman (1980) proposed the use of a home-range estimator based on the harmonic mean of a bivariate data set that places the center of activity in the area of greatest activity. The peeling algorithm is as above but where c is calculated as follows:

$$\text{Let } s_j = \frac{1}{\frac{1}{n}\sum_{i=1, i\neq j}^{n} \frac{1}{[(x_i - x_j)^2 + (y_i - y_j)^2]^{1/2}}}$$

for all i, and where $(x_i, y_i) \neq (x_j, y_j)$ (7)

Let $s_j^* = \text{argmin} s$(i.e., the value of j that minimizes s); thus, $c = (x_j^*, y_j^*)$. Note that c is 1 of the locations of the data (Spencer and Barrett 1984 cited in Kenward 1987) and does not suffer from some of the problems associated with other implementations of the harmonic mean (e.g., Dixon and Chapman 1980).

Peeling point that causes the greatest decrease in area.—For each iteration, we removed the location that caused the greatest difference in area between the MCP of the data set with and without this point. That is, let A_{MCP} represent the area of the MCP of the current, remaining data, and let $A_{MCP\text{-}i}$ represent the area of the MCP of the current, remaining data minus the ith location. For each iteration, our objective was to find the location i, to maximize $A_{MCP} - A_{MCP\text{-}i}$. Fortunately, we did not need to test all points in the current data, the most extreme points were, by definition, those that made up the MCP. Thus, for each iteration, our set of candidate locations was restricted to those points that comprised the MCP. As before, we removed the selected location from the data and repeated the process as desired (e.g., White and Garrott 1990). For instance, if we desire the 50% MCP, we peel until the outer 50% of points have been removed (e.g., Worton 1995).

Expected Properties of UD Curves

We assessed the 3-point peeling methods by comparing UD curves obtained from simulated data. Our procedure was 1) we simulated data from 1 of the 5 distributions described earlier, 2) we peeled locations using 1 of the 3 criteria, and 3) we obtained the UD curve. We repeated this procedure for each peeling method and all 5 distributions. Ideally, these comparisons should expose potential strengths and/or weaknesses of each method in determining the underlying distribution or core area of a set of locations.

Scaling the polygon areas in the utilization distribution (y-axis) is necessary since even a few extreme outliers can radically affect the plots of UD curves. Without scaling, the curves become difficult to compare across datasets and distributions. Cairns (2001) notes 2 plausible scaling methods. The first method, used by Kenward (1987) and Anderson (1998), divides each polygon area by the largest hull area, the MCP. This method has the advantage of condensing all data into a standardized, fixed-scale plot that is easily comparable to other data UD curves. A problem with this method, however, is its lack of robustness. Extreme outliers can affect the shape of the curve and thus obscure the underlying distribution or core area. A second scaling procedure divides the area of each polygon by the area containing the central 50% of all data fixes (Worton 1995, Hatchwell et al. 2001). For example, the centroid point peeling method would use as a scaling factor the area containing the 50% of data points closest in distance to the data set's centroid.

Worton (1995) notes the robustness of the 50% polygon peel. That is, most outliers are removed from a dataset once the outer 50% of data points have been removed. As such, it is considered an attractive alternative to the MCP standardizing method. Other useful properties include (Hatchwell et al. 2001):

1. The shape of the UD curve suggests where the animal or group is spending its time. For groups that utilize their home ranges uniformly, a linear relationship between the proportion of fixes and standardized polygon areas is expected. This relationship is represented by a straight line from the origin passing through (0.5, 1) to (1, 2; Fig. 2a). We refer to this group's utilization

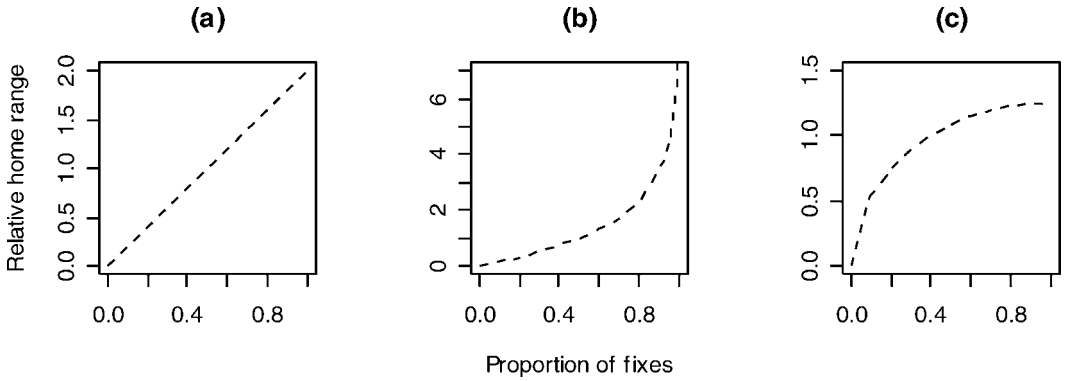

Figure 2. Simulated relationships between relative home-range area and peel level for groups that: (a) occupy their range uniformly, (b) avoid peripheral areas or prefer core areas, and (c) behave territorially. Note differences in scale of *y*-axis.

line as the reference line. A group that tends to avoid home-range boundary regions will also have a distinguishable curve. The boundary will have relatively low density of locations and, as these are peeled off, the area will decrease relatively rapidly. As the peels reach the denser core, this rate will decrease and result in a concave curve that passes above the reference line beyond the point (0.5, 1; Fig. 2b). Alternatively, a more territorial group spending much time at its home-range boundary regions will have a convex curve that bows above that of the reference line (Fig. 2c). The density of points should be lower in the smaller, central polygon areas and higher with increasing polygon area.

2. The loss of a distinct cluster of fixes from a subsequent polygon peel will appear as a kink in the curve. This is because the loss of a cluster is likely to cause a significant decrease in the area of the subsequent polygon peel, but it will cause only a small decrease in the proportion of fixes in the remaining data set (Kenward 1987, Anderson 1998, Hatchwell et al. 2001).

Expected curves: MAP(p) function.—The UD curve, a plot of hull areas versus cumulative density, is essentially a cumulative distribution function, although the UD curve has some disparity at the extreme ends of each curve (Anderson 1998, Cairns 2001). As such, it would be possible to determine the (asymptotic) expected curve for some of the distributions described in section 2. Worton (1995) refers to the unscaled expected curves as functions of minimum area containing probability $p \in [0,1]$ of the utilization distribution, denoted $MAP(p)$.

To obtain the expected curves for each of the distributions, we first calculated the corresponding $MAP(p)$ function. In many cases, especially with the circular distributions that we considered, it made sense to derive the *MAP* functions using polar rather than Cartesian coordinates. More generally, one can argue that data are limited in space; therefore, data can fit crudely within a circle, so the coordinate conversion is appropriate. To convert from Cartesian to polar coordinates we used the following relationships:

$$s^2 = x^2 + y^2 \quad \text{and} \quad \theta = arctan(y/x). \tag{8}$$

where s is the radial distance from the origin, and θ is the counterclockwise angle from the x-axis.

The limits of the distributions must also be converted. For the radial component, $s \in [0, r]$, and for the angular component, $\theta \in [0, 2\pi]$. Once the probability density function was redefined in polar coordinates, we found the marginal density function of the radial component by integrating over the entire range of θ:

$$f(s) = \int_0^{2\pi} f(s, \theta) d\theta. \tag{9}$$

The marginal cumulative distribution function for the radial component is:

$$F(s) = \int_o^r f(s) ds. \tag{10}$$

The function $F(s)$ equated probability with radius. Expressing the probability, p, in terms of the radius, r, yielded an expression that related radius to probability level. We could then determine the area of the polygon given the value of the radius, r.

Cairns (2001) gives detailed derivations of expected curves for various distributions. We used the $MAP(p)$ functions for 2 distributions (Table 1). We then scaled the $MAP(p)$ functions by dividing by the 50% area (i.e., the value of $MAP(0.5)$; Table 1).

Unfortunately, it was not possible to obtain an explicit, exact $MAP(p)$ function for the other 3 distributions. For the skewed bivariate distribution, there is no closed form expression of the joint cumulative distribution function of a nonstandard bivariate normal distribution. We could not obtain an explicit function for the cluster process since it is based on a Poisson process that does not have a single, defining probability density function. Finally, while there exists a closed form of the joint cumulative distribution function of the inverted bivariate normal distribution:

$$p = \frac{2\pi}{c}\left(\exp\left(-\frac{r^2}{2}\right) + \frac{r^2}{2} - 1\right), \tag{11}$$

Table 1. *MAP*(*p*) and *MAP*(*p*) / *MAP*(0.5) functions for the uniform on a disk, standard, and inverted bivariate normal distributions.

Distribution	MAP(p)	*MAP*(*p*) / *MAP*(0.5)
Uniform on a disk of unit radius	π p	2 p
Standard bivariate normal	$-2\ \pi \log(1 - p)$	$-\log(1 - p) / \log 2$
Inverted bivariate normal	$\approx \pi\sqrt{4cp/\pi}$	$\approx \sqrt{2p}$

it is not possible to write r in terms of $f(p)$ exactly. However, we can approximate it. That is, taking the first 3 terms of the MacLaurin series:

$$\exp\left\{\frac{-r^2}{2}\right\} \approx 1 - \frac{r^2}{2} + \frac{r^4}{8} + \cdots, \quad (12)$$

then:

$$p \approx \frac{2\pi}{c}\left(1 - \frac{r^2}{2} + \frac{r^4}{8} + \frac{r^2}{2} - 1\right), \quad (13)$$

which can be rearranged to obtain:

$$r^2 \approx \sqrt{4cp/\pi}. \quad (14)$$

Figure 3 shows the expected curves of the scaled $MAP(p)/MAP(0.5)$ functions. Numerical methods were used to obtain the curve for the skewed distribution when $\alpha = 2$, 3, and 4 (Fig. 3*b*).

The similarity in expected curves of the 3 skewed distributions (Fig. 3*b*) was a result of the centroid's decreasing value along the x coordinate as skew increased (Equation 6). The increase in skew lead to a larger 50% polygon peel that, in turn, decreased the y-axis values on the plot of UD curves. This, in effect, tended to standardize the curves.

UD curves from simulated data.—For each point peeling method, we simulated 50 samples of $n = 100$ fixes from each distribution. There was potential for ≥ 2 locations to be identical when data were discretized (e.g., an animal's x or y coordinate was rounded to the nearest m, km, etc.) or when an animal repeatedly returned to the same location (e.g., nest or den). If we superimposed locations, the peeling methods we outlined may not work properly. This issue is easily addressed by jittering the data by adding a small amount of random noise to each location—ideally from a circular distribution such as uniform on a disk (Cairns 2001) in which the size of this noise distribution is a small proportion (0.1%) of the range of the sample data to which it is applied. This procedure of jittering is advised by Anderson (1998) and Cairns (2001), as it ensures that even if an individual has visited a particular site a number of times, these locations are distinguishable, and the appropriate weight is given to the site when peeling. This is not an issue when simulating data from known distributions, as we did, since the x and y coordinates are real, in other words not discretized.

Uniform on a disk.—The UD curves of the uniform distribution on a disk, using the centroid peeling function, lie closely along the line $y = 2x$ from the point (0, 0) to (1, 2; Fig. 4i[a]). Comparable curves were obtained using the harmonic mean (Fig. 4i[b]) and greatest decrease in area (Fig. 4i[c]) point peeling functions.

Bivariate normal distribution.—Utilization distribution curves for the bivariate normal distribution were obtained using the centroid peeling function (Fig. 4ii[a]), harmonic mean peeling function (Fig. 4ii[b]), and greatest decrease in area peeling function (Fig. 4ii[c]). As noted in section 2, this distribution would be representative of a group that avoided the boundary regions of its home range and instead tended to move within a core (mononuclear) area. Again, all 3 methods generated similar curves. All reflected concavity and passed above the reference line beyond the point (0.5, 1). The harmonic mean curves, however, displayed greater variation compared to curves obtained from the other methods.

To assess the larger variation found among curves of the harmonic mean method, we simulated $n = 100$ locations for $N = 300$ samples from the bivariate standard normal distribution for the (*a*) centroid and (*b*) harmonic mean methods (Fig. 5). We calculated and plotted the centroid and harmonic mean centers for each simulation. We noted a markedly larger spatial variance exhibited by the harmonic mean method (Fig. 5b). A possible explanation for this occurrence may be found in the properties of the harmonic mean in which the identified center can shift widely depending on where most data points were located at any given time (Dixon and Chapman 1980). The harmonic mean center was always located within the densest region of the home range. As such, the harmonic mean center will always show greater variability compared to the centroid due to its sensitivity to internal data locations.

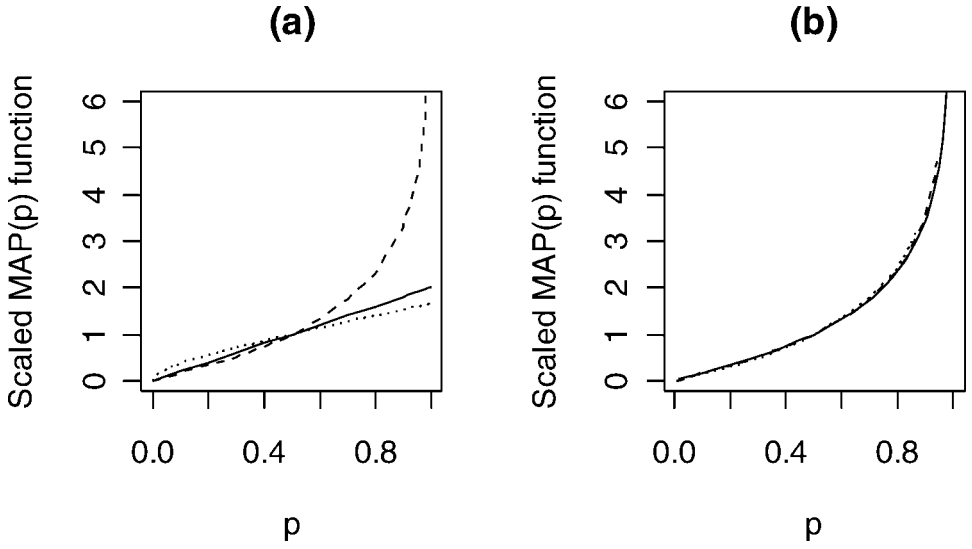

Figure 3. *MAP*(*p*) / *MAP*(0.5) functions (scaled expected curves) for (a) the uniform on a disk (solid line), bivariate normal (dashed), and inverted bivariate normal (dotted) distributions, and (b) skewed distributions where $\alpha = 2$ (solid line), $\alpha = 3$ (dashed), and $\alpha = 4$ (dotted).

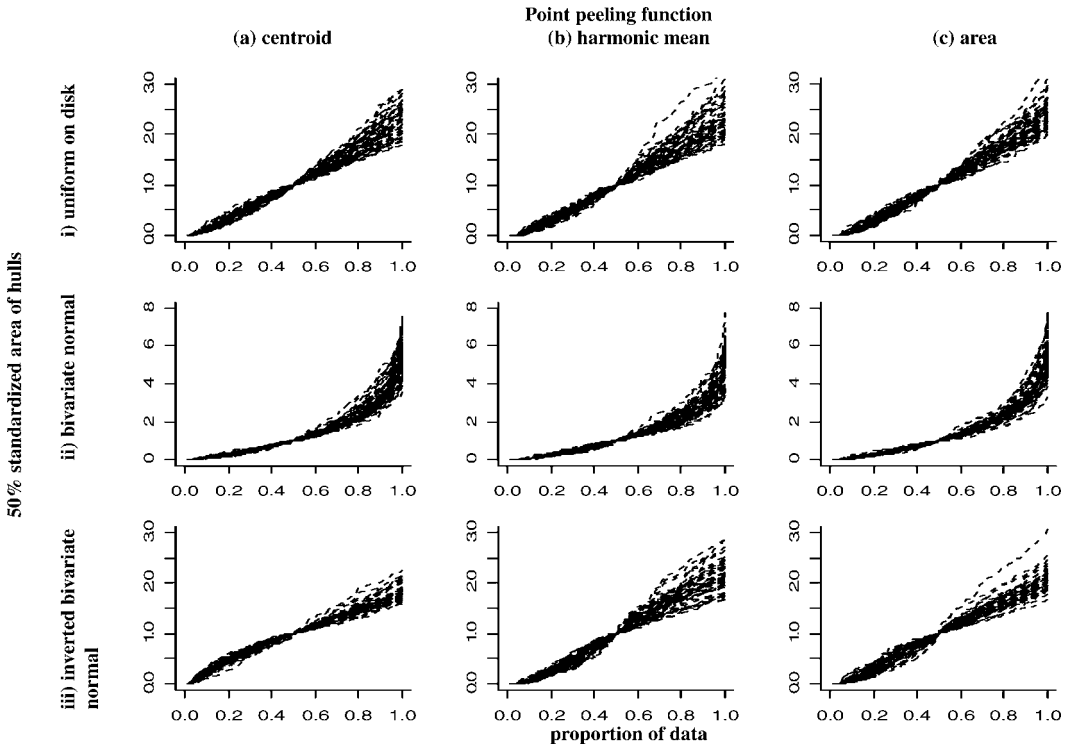

Figure 4. The UD curves where $n = 100$ and $N = 50$ from the distributions (i) uniform on a disk, (ii) bivariate normal, and (iii) inverted bivariate normal ($m = 3$) using the (a) centroid, (b) harmonic mean, and (c) greatest decrease in area peeling functions.

Inverted bivariate normal distribution.—As stated above, we expected the UD curves of a group moving around the periphery of its home range to be bowed above the uniform distribution reference line. The inverted normal distribution represents this type of territorial behavior. The UD curves from an inverted bivariate normal distribution using the centroid peeler show the expected bowing, but it is not pronounced (Fig. 4iii[a]). This may be because the parameter representing the territorial nature of the group is at an intermediate value ($m = 3$). When representation of territorial behavior is increased in this distribution (larger m), the signature bowing becomes more apparent. Further, it is clear that the 50% hull area was relatively large and the standardized area values (y-axis) relatively small compared to those of the bivariate normal distribution curves. Thus, the UD curve of this distribution had 2 distinguishable features: 1) the convexity above the reference line, and 2) the smaller y values relative to distributions with a core density.

The harmonic mean curves did not show a similar trend (Fig. 4iii[b]). In fact, there was greater among curves compared to those of the centroid peeling function. Since the central region of this distribution contains so few fixes, the location of the harmonic mean can vary widely (Fig. 6). For example, 1 sample simulation may have mild clustering in 1 region of the home range that will pull the harmonic mean toward it. Another sample simulation, using the same parameters, may exhibit a slightly denser region elsewhere, thus displaying a harmonic mean far from that of the first simulation. This variance would, of course, translate to increased variance among the utilization curves. Thus, the harmonic mean peeler may not be the most effective method for uncovering this type of distribution.

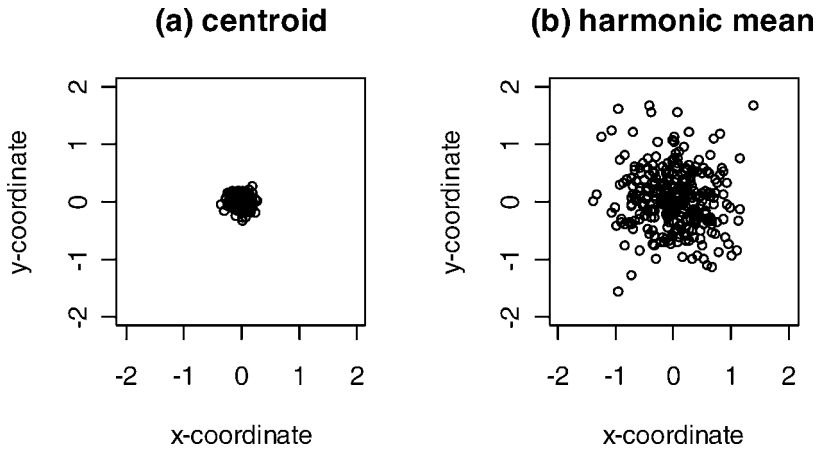

Figure 5. (a) Centroid values and (b) harmonic mean values for the bivariate normal distribution with $n = 100$ locations ($N = 300$ replicates).

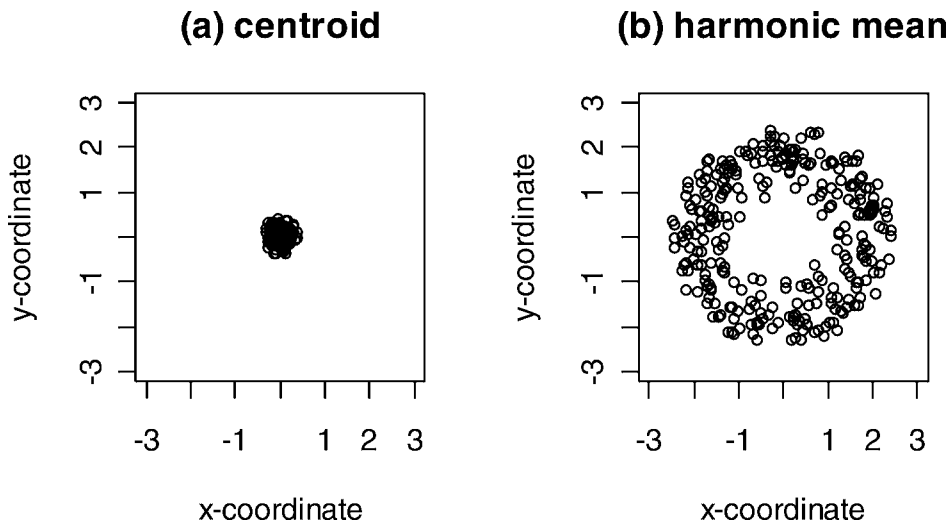

Figure 6. (a) Centroid values and (b) harmonic mean values from the inverted bivariate normal distribution with $n = 100$ locations ($N = 300$ replicates).

Like the harmonic mean peeler, the area peeler did not reveal any distinguishable, expected features in the UD curves of the inverted bivariate normal distribution. This may be because the area peeler was specifically designed to drop points based on large decreases in MCP areas. Thus, as the points near the interior were dropped, a significant drop in area may occur quickly and be followed by an almost negligible drop in area for the remaining points (as in Fig. 4iii[c]).

Skewed distribution.—Utilization distribution curves from all peeling functions exhibit the signature concave bowing of a distribution containing a single core area (Fig. 7i). In fact, based on our data, the UD curves of the skewed bivariate distribution and the symmetric bivariate distribution were almost indistinguishable. However, the *y*-axis values of the skewed distribution's UD curves were generally smaller than those of the symmetric bivariate distribution. This was to be expected since the 50% polygon area will be larger for a skewed distribution, so the standardized *y*-axis values will be smaller. Unfortunately, the *y*-axis values for the skewed and symmetric distributions overlapped greatly, so determining the correct underlying distribution is still difficult.

Once again, the harmonic mean curves displayed a significant

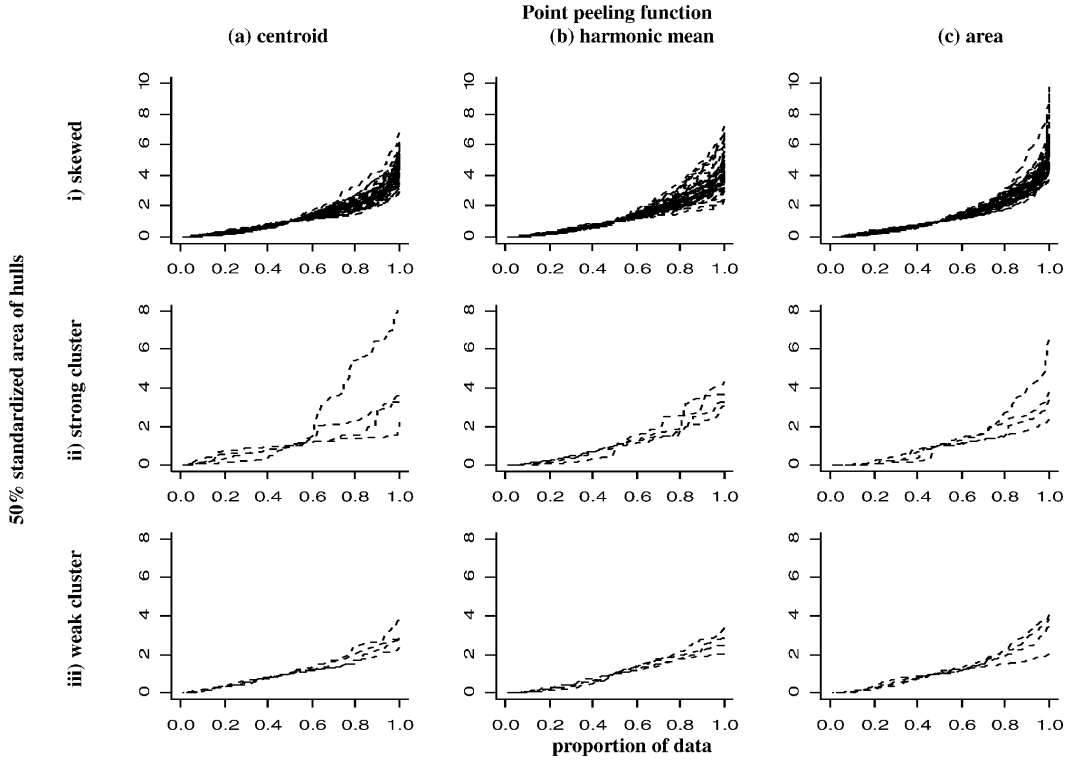

Figure 7. The UD curves where $n = 100$ and $N = 50$ from the (i) skewed distribution (skew = 4), (ii) Thomas cluster process (strong clustering where $\lambda = 2$, $\sigma = 0.1$, $\mu = 50$, $m = 3$), and (iii) Thomas cluster process (weak clustering where $\lambda = 2$, $\sigma = 0.2$, $\mu = 50$, $m = 3$) using the (a) centroid, (b) harmonic mean, and (c) greatest decrease in area peeling functions.

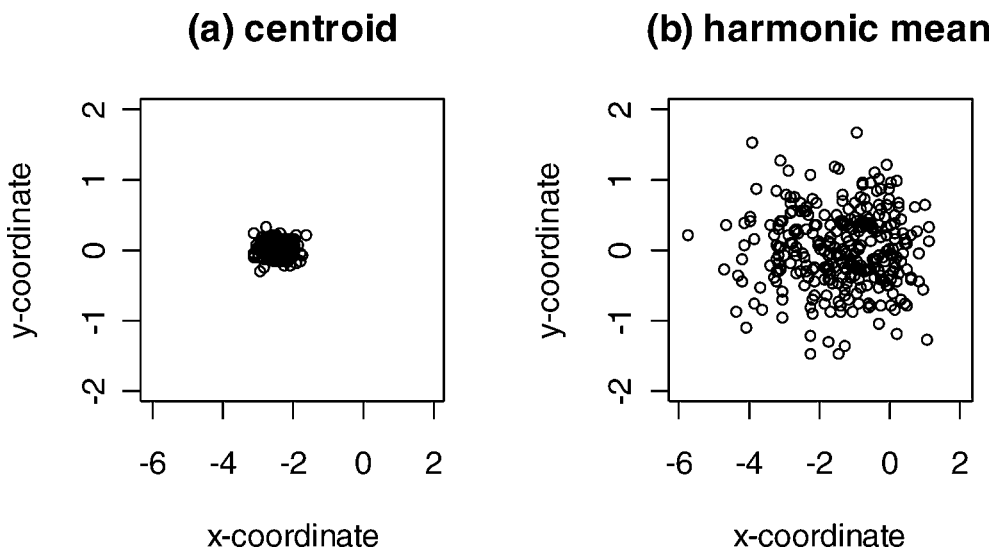

Figure 8. (a) Centroid values and (b) harmonic mean values for the skewed bivariate distribution with $n = 100$ locations ($N = 300$ replicates).

variation (Fig. 7i[b]). A plausible explanation for this large variation is that the wide range of possible locations for the harmonic mean lead to increased variance among the utilization curves (Fig. 8).

Thomas cluster process.—The curves we generated using the Thomas cluster process (Fig. 7ii[a,b,c]) revealed a distinguishable pattern. There were kinks in the curves that were not apparent in other UD curves; this is an extremely useful feature of the UD curve. First, we derived UD curves from a simulated data set having strong clustering parameters (Fig. 7ii). The characteristic kinks were displayed best by the centroid and harmonic mean point peeling functions. The greatest drop in area function tended to display smoother curves. This made sense intuitively since the area function excluded points one at a time based on the largest drop in polygon area. Consecutively peeled points would most likely not be contained in the same cluster; thus, the large drops in area (or kinks) would not occur as often. The points would be removed in a more random fashion relative to the centroid or harmonic mean point peelers.

In contrast, UD curves were also derived from a simulated data set having weak clustering parameters (Fig. 7iii[a,b,c]). Although some kinks were apparent in the centroid and harmonic mean curves, overall, these curves were not as clearly distinguishable as those derived from a simulated data set with strong clustering parameters (Fig. 7ii). We expected this since kinks in the curves were formed when specific clusters were peeled off. The more distinct the clusters, the more distinct the kinks in UD curves. Again, the centroid and harmonic mean curves displayed the kinks more clearly than did the area peeler curves.

The harmonic mean function showed significant variation, however, when comparing the simulated centroid and harmonic mean center points (Fig. 9), which possess a comparable amount of variation.

Conclusions.—We found that the centroid peeler was the most consistent and reliable method by which to assess the underlying distribution of a sample of fixes. While the area peeler did well with the bivariate standard normal distribution, it did not accurately reflect the inverted bivariate normal distribution or cluster process. The harmonic mean function consistently exhibited high variability that can be attributed to the high spatial variability found in the simulated harmonic mean centers. This variability could possibly lead to misrepresentation of an underlying distribution.

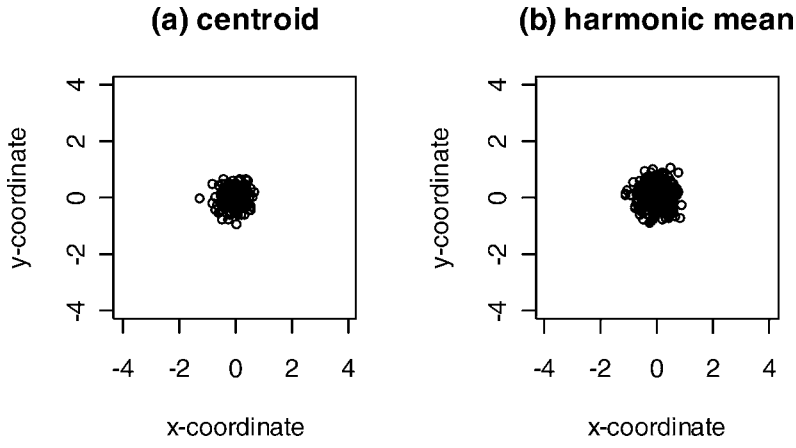

Figure 9. (a) Centroid values and (b) harmonic mean values for the Thomas cluster process with $n = 100$ locations ($N = 300$ replicates).

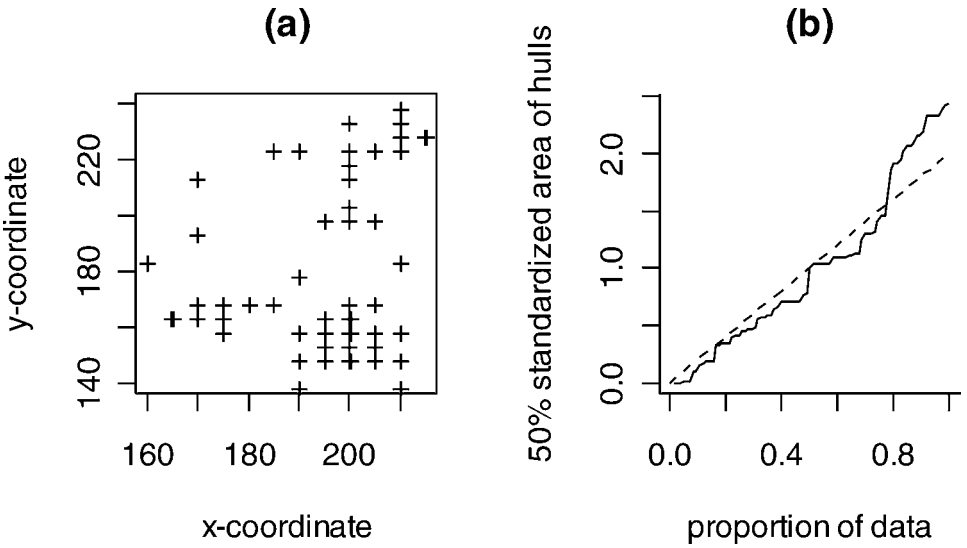

Figure 10. (a) Utilization distribution of wood mouse Indigo (Macdonald et al. 2000), (b) UD curve (solid line) and expected curve for a uniform distribution on a disk (dashed).

None of the 3-point peeling methods clearly differentiated between a skewed and symmetric bivariate normal distribution. Also, the signature kinks in UD curves for the Thomas cluster process became less visible with weaker clustering data.

Analysis of Empirical Data

As an illustration and test of the above methods, we analyzed 5 samples from actual field studies. We used the centroid point peeling function to calculate all UD curves because we found that it offered the most accurate, consistent results.

To represent uniform home-range use, we used a plot of fixes for an individual wood mouse (*Apodemus sylvaticus*) named Indigo (Macdonald et al. 2000; Fig. 10a). Its behavior, and thus the most closely matching statistical distribution, was not entirely apparent based on this plot. The corresponding UD curve (Fig. 10b), however, revealed a uniform pattern of movement (alternatively interpreted as random set of fixes) with a reduced density on the margins.

Skewed home-range use was represented by home-range fixes of a group of elk (*Cervus elaphus*; Millspaugh 1999; Fig. 11a). This plot shows that there was considerable skew in home-range use. It is difficult to determine, however, whether a central core existed or whether clustering occurred in certain regions. The UD curve (Fig. 11b) offered a much clearer interpretation. The concavity of the curve depicted a skewed distribution, while the relatively small *y*-axis values suggested a wide 50% core area. The lack of kinks in the UD curve suggested little or no clustering.

A sample of fixes from an individual wood mouse named Vermillion was used to represent clumped home-range usage (Macdonald et al. 2000; Fig. 12a). This plot appears to represent a species with underdispersed point locations. The UD curve (Fig. 12b) verifies this observation. Kinks in the UD curve suggest a clustering of fixes in several regions throughout the home range.

Utilization distributions of mule deer locations from 2 consecutive years (White and Garrott 1990) compared skewed and

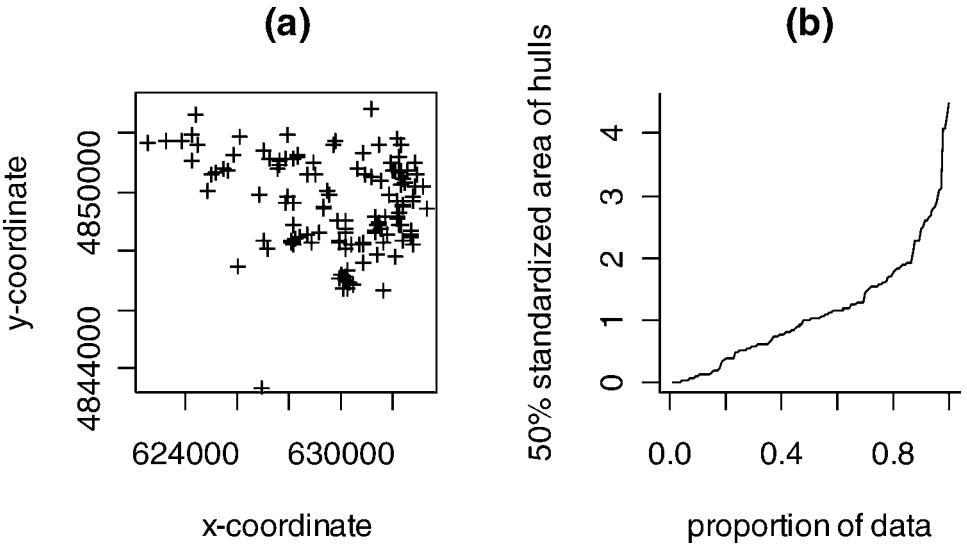

Figure 11. (a) Utilization distribution of elk data (Millspaugh 1999), (b) UD curve.

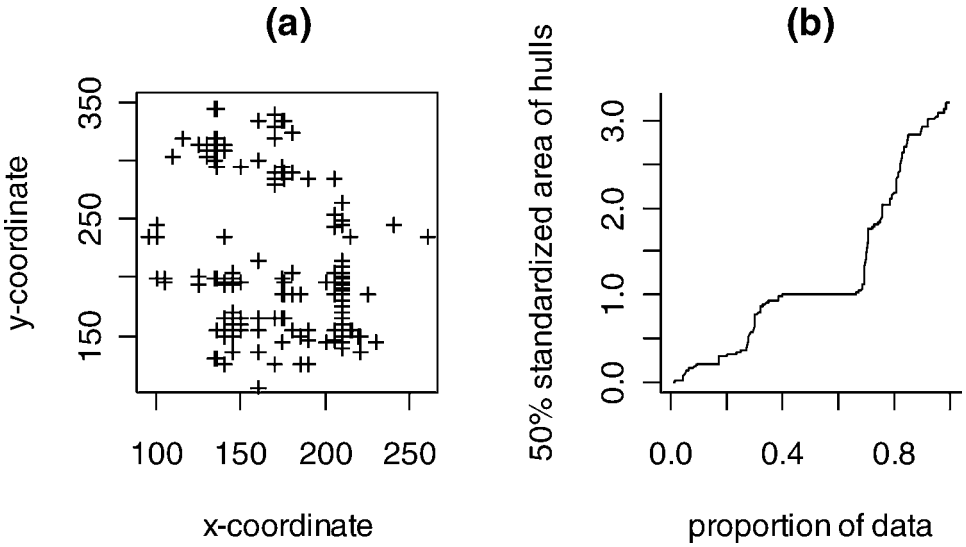

Figure 12. (a) Utilization distribution of wood mouse Vermillion (Macdonald et al. 2000), (b) UD curve.

uniform home-range use from the same study site (Fig. 13a,b). A visual interpretation of these 2 plots suggested that each has a skewed underlying distribution. The UD curves of the 2 distributions (Fig. 13c), however, reveal a different interpretation; the concavity of a skewed distribution's UD curve is apparent in the 1985 data. The UD curve of the 1984 data suggested a uniform distribution instead. That is, the slight skew in the 1984 data (Fig. 13a) is not enough to discount the possibility of a uniform underlying distribution.

Discussion

The centroid peeler offered the most accurate and consistent results, and the UD curves generated with this method were consistent in shape with expected curves. This peeler method also performed well in identifying clusters in simulated home ranges containing heavy or medium amounts of clustering. We believe the centroid peeler's high performance was due to its tendency to remain stable throughout all samples.

Utilization distribution curves generated by the harmonic mean peeler exhibited particularly large amounts of variability, mostly attributable to the instability of the harmonic mean center. This stands to reason since the harmonic mean center was always located within the densest region of the home range. Importantly, this variability could lead to misrepresentation of an underlying behavior. Further, the UD curves of the harmonic mean peeler did not identify the inverted bivariate normal distribution representing territorial behavior.

Unlike the harmonic mean peeler, UD curves of the area peeler did not exhibit as much variability; in fact, variability matched that of the centroid peeler. However, the area peeler curves were not able to identify clustering or territorial behavior. Since the area peeler function excluded points one at a time based on the largest drop in polygon area, peeled points would most likely not be contained in the same cluster. As such, large drops in areas (or kinks) would not occur as often.

None of the 3 peeler functions clearly differentiated between a symmetric and skewed distribution. Although the *y*-axis values were smaller for a skewed rather than symmetric distribution, the curves showed a large amount of overlap in these values for the 2 distributions. Thus, it will still be difficult to determine the most likely behavior and, hence, the most closely matching and appropriate statistical distribution. However, an animal's home range is rarely represented by a perfectly symmetric bivariate normal distribution.

The 3 peelers also had difficulty identifying weak clustering behavior. This is not surprising since the signature kinks found in

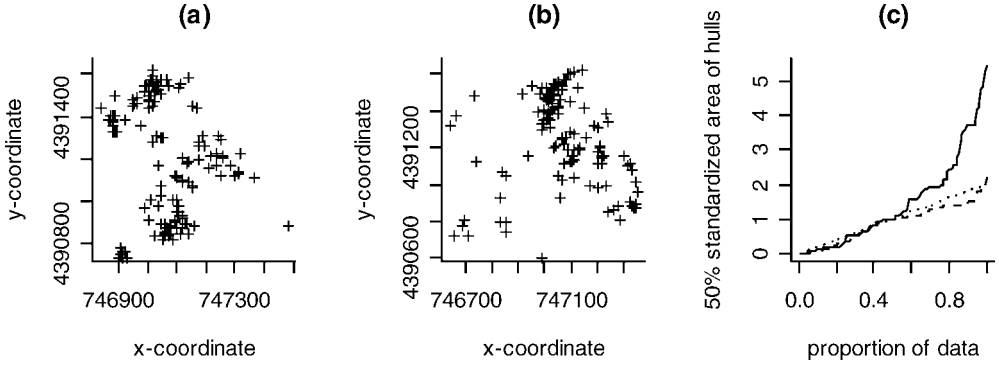

Figure 13. Mule deer home-range fixes (White and Garrott 1990), (a) 1984 data, (b) 1985 data, and (c) UD curves for 1984 (dashed line), 1985 (solid), and expected curve for uniform on a disk (dotted).

UD curves of a cluster process are formed when an entire cluster is peeled from the sample. The more distinct the cluster, the more distinct the kinks in UD curves. Weakly clustering groups would be represented by smoother curves with less pronounced, if any, kinks.

We found the centroid peeler to be the most appropriate peeling function when assessing UD curves to determine the underlying distribution of a home-range sample. We addressed our second objective (i.e., comparison of sample and expected UD curves as the basis of a procedure for classifying animal behavior) by comparing sample data to expected UD curves using the centroid peeler. Given our results, the point peeling method we described using the centroid peeling function offered a quantitative and objective approach to assessing animal home range.

We found that point peeling provided a simple but robust procedure for field biologists that made good use of all the data from a sample, provided an objective home-range measure, and provided a way of classifying home-range use. An extension is convex hull peeling. In contrast to point peeling, hull peeling essentially peels extreme locations in all directions simultaneously but does not rely on an arbitrary center such as the centroid. As with point peeling, however, the area of the remaining data is calculated at each iteration to produce a UD curve. Earlier work (Green 1981, Anderson 1998, Hatchwell et al. 2001, see also Getz and Wilmers 2004) indicates that convex hull peeling has some favorable statistical properties; thus, we recommend replicating our study with convex hull peeling to determine whether it does provide better performance than point peeling.

Management Implications

A better understanding and estimate of the home range of an animal or population have significant implications for management. First, home-range data (size, shape, overlap) can provide significant insights into basic life history and sociality of a species or population (Galbraith et al. 1987). For instance, such data can elucidate differences among adults and juveniles, difference between the sexes, and existence of philopatry. Second, the home range identifies a particular patch of habitat and this, again, not only provides important information about a population's ecology—including dietary needs—but can also be a gauge of habitat quality. That is, variation in home range among individuals or a trend of increasing home range versus time could be an important measure of habitat quality or habitat degradation (e.g., Johnson et al. 2000, Pejchar et al. 2005), and an increase in overlap of home ranges and presence of helping behavior could be a strong indicator of resource limitation. An example is the sociality change that occurred when the Seychelles brush warbler (*Acrocephalus sechellensis*) was reintroduced to Aride Island (Komdeur 1992): with the initial low population density, adults and juveniles lived relatively separate lives with little home-range overlap, but as the island space-limited population grew, juveniles became increasingly likely to stay within the bounds of their parent's home range until a territory became vacant. Finally, armed with such detailed biological and ecological understanding, conservation biologists, land-use planners, and other practitioners are in a far better position to design reserves (e.g., use such data to justify minimum reserve size and the need for certain habitat corridors), plan and execute monitoring programs (e.g., to monitor whether animals are remaining within the reserve bounds and to monitor reinvasion and population recovery of a pest or actively controlled species), and protect and manage the animals (e.g., the assignment of rangers to specific areas).

Acknowledgments

We thank the following for permission to use their empirical data: J. Millspaugh for the Black Hills elk data from his dissertation; G. White and R. Garrott for the mule deer data from the Piceance Basin study; and D. Macdonald for the wood mice data, who in turn gratefully acknowledges Natural Environment Research Council funding, especially from the Joint Agriculture and Environment Programme. Our study was generously supported by funds from Georgia Institute of Technology's Institute for Sustainable Technology and Development. We thank the director, B. Bras, for his financial and moral support.

Literature Cited

Alcock, J. 1998. Animal behavior. Sixth edition. Sinauer, Sunderland, Massachusetts, USA.

Anderson, C. 1998. The organisation of foraging in insect societies. Dissertation, University of Sheffield, Sheffield, United Kingdom.

Baddeley, A., and R. Turner. 2005. Open source software for spatial statistics. <http://www.spatstat.org/>. Accessed 2005 Dec 2.

Boulanger, J. G., and G. C. White. 1990. A comparison of home-range estimators using Monte Carlo simulation. Journal of Wildlife Management 54: 310–315.

Burt, W. H. 1943. Territoriality and home range concepts as applied to mammals. Journal of Mammology 24:346–352.

Cairns, D. A. 2001. Measuring range and assessing interaction through radio-telemetry. Thesis, University of Sheffield, Sheffield, United Kingdom.

Dixon, K. R., and J. A. Chapman. 1980. Harmonic mean measure of animal activity areas. Ecology 6:1040–1044.

Ford, R. G., and D. W. Krumme. 1979. The analysis of space use patterns. Journal of Theoretical Biology 76:125–155.

Franks, N. R. 1989. Army ants: a collective intelligence. American Scientist 77: 139–145.

Galbraith, D. A., M. W. Chandler, and R. J. Brooks. 1987. The fine structure of home ranges of male *Chelydra serpentina*: are snapping turtles territorial? Canadian Journal of Zoology 65:2623–2629.

Getz, W. M., and C. C. Wilmers. 2004. A local nearest-neighbor convex-hull construction of home ranges and utilization distributions. Ecography 27: 489–505.

Gibson, R. M., and J. W. Bradbury. 1987. Lek organization in sage grouse: variations on a territorial theme. The Auk 104:77–84.

Green, P. J. 1981. Peeling bivariate data. Pages 3–19 *in* V. Barnett, editor. Interpreting multivariate data. Wiley, New York, New York, USA.

Hatchwell, B. J., C. Anderson, D. J. Ross, M. K. Fowlie, and P. G. Blackwell. 2001. Social organization of cooperatively breeding long-tailed tits: kinship and spatial dynamics. Journal of Animal Ecology 70:820–830.

Hayne, D. W. 1949. Calculation of size of home range. Journal of Mammalogy 30:1–18.

Hodder, K. H., R. E. Kenward, S. S. Walls, and R. T. Clarke. 1998. Estimating core ranges: a comparison of techniques using the common buzzard (*Buteo buteo*). Journal of Raptor Research 32:82–89.

Johnson, D., R. Kays, D. W. Macdonald, and P. G. Blackwell. 2000. Does the resource dispersion hypothesis explain group living? Trends in Ecology and Evolution 17:563–570.

Kenward, R. E. 1987. Wildlife radio tagging—equipment, field techniques and data analysis. Academic, London, United Kingdom.

Kenward, R. E. 2001. A manual for wildlife radio tagging. Academic, London, United Kingdom.

Kernohan, B. J., R. A. Gitzen, and J. J. Millspaugh. 2001. Analysis of animal space use and movements. Pages 125–166 *in* J. J. Millspaugh, and J. M.

Marzluff, editors. Radio tracking and animal populations. Academic, San Diego, California, USA.
Komdeur, J. 1992. Importance of habitat saturation and territory quality for evolution of cooperative breeding in the Seychelles warbler. Nature 358: 493–495.
Macdonald, D. W., T. E. Tew, I. A. Todd, J. P. Garner, and P. J. Johnson. 2000. Arable habitat use by wood mice (*Apodemus sylvaticus*). 3. A farm-scale experiment on the effects of crop rotation. Journal of Zoology 250: 313–320.
Millspaugh, J. J. 1999. Behavioral and physiological responses of elk to human disturbances in the southern Black Hills, South Dakota. Dissertation, University of Washington, Seattle, USA.
Orians, G. H., and N. E. Pearson. 1979. On the theory of central place foraging. Pages 154–177 *in* D. J. Horn, R. D. Mitchell, and G. R. Stairs, editors. Analysis of ecological systems. Ohio State University, Columbus, USA.
Pejchar, L., K. D. Holl, and J. L. Lockwood. 2005. Hawaiian honeycreeper home range size varies with habitat: implications for native *Acacia koa* forestry. Ecological Applications 15:1053–1061.
Powell, R. A. 2000. Animal home ranges and territories and home range estimators. Pages 65–110 *in* L. Boitani, and T. K. Fuller, editors. Research techniques in animal ecology: controversies and consequences. Columbia University Press, New York, New York, USA.
Spencer, W. D., and R. H. Barrett. 1984. An evaluation of the harmonic mean method for evaluating carnivore activity areas. Acta Zoologica Fennica 171: 255–259.
Seaman, D. E., and R. A. Powell. 1996. An evaluation of the accuracy of kernel density estimators for home range analysis. Ecology 77:2075–2085.
Stephens, D. W., and J. R. Krebs. 1986. Foraging theory. Princeton University Press, Princeton, New Jersey, USA.
Stewart, P. D., C. Anderson, and D. W. Macdonald. 1997. A mechanism for passive range exclusion: evidence from the European badger (*Meles meles*). Journal of Theoretical Biology 184:279–289.
Van Stralen, G. E. 1998. Home range size and habitat use of urban black bears in southern California. Thesis, California State University, Northridge, USA.
White, G. C., and R. A. Garrott. 1990. Analysis of wildlife radio-tracking data. Academic, San Diego, California, USA.
Worton, B. J. 1995. A convex hull-based estimator of home-range size. Biometrics 51:1206–1215.
Wray, S., W. J. Cresswell, P. C. L. White, and S. Harris. 1992. What, if anything, is a core area? An analysis of the problems of describing internal range configurations. Pages 256–271 *in* I. G. Priede, and S. M. Swift, editors. Wildlife telemetry: remote monitoring and tracking of animals. Ellis Horwood, New York, New York, USA.

Appendix A. Sample generation.

So that our results might be replicated, we detail the methodology by which we generated n sample deviates for each of our 5 distributions:

(1) Uniform distribution: we used a rejection technique: $X,Y \sim U(-1,1)$, accepting coordinate pairs for a sample if $x^2 + y^2 + 1$, rejecting otherwise.

(2) Bivariate normal: in Splus, this can be simulated using standard functions: X, $Y \sim$ rnorm(1,0,1).

(3) Inverted bivariate normal: we used the following rejection-based algorithm:

$i \leftarrow 0$
while ($i \leq n$) {
  $X,Y \sim U(-\sigma, \sigma)$
  if ($x^2 + y^2 \leq \sigma$){
    if ($U(0,1) > \exp\{-(x^2+y^2)/2\}$) then $(x_i,y_i) \leftarrow (x,y)$; $i \leftarrow i+1$
  }
}

(4) Skewed distribution:

for (i in 1:n) {
  if $U(0,1) \leq 1/(\alpha + 1)$ then $(x_i,y_i) \leftarrow (-|x|,y) \sim N(0,0,1,1,0)$
  otherwise$(x_i,y_i) \leftarrow (-|x|,y) \sim N(0,0,\alpha,1,0)$
}.

(5) Multilocus clustered distribution: we used the rThomas routine of the 'SPATSTAT' library, rThomas(λ, σ, μ, owin(c(0,1),c(0,1))), and we took the n closest locations (in 2D Euclidean distance) to the centroid.

Associate Editor: White.